Orbital-selective formation of local moments in α-iron: First-principles route to an effective model

A. A. Katanin, A. I. Poteryaev, A. V. Efremov, A. O. Shorikov, S. L. Skornyakov, M. A. Korotin, and V. I. Anisimov
Institute of Metal Physics, Russian Academy of Sciences, 620041 Yekaterinburg GSP-170, Russia
(Received 19 October 2009; revised manuscript received 7 December 2009; published 14 January 2010)

We revisit a problem of theoretical description of α-iron. By performing local-density approximation plus dynamical mean-field theory calculations in the paramagnetic phase we find that Coulomb interaction and, in particular, Hund exchange, yields the formation of local moments in e_g electron band, which can be traced from imaginary-time dependence of the spin-spin correlation function. This behavior is accompanied by non-Fermi-liquid behavior of e_g electrons and suggests using local-moment variables in the effective model of iron. By investigating orbital-selective contributions to the Curie-Weiss law for Hund exchange $I=0.9$ eV we obtain an effective value of local moment of e_g electrons $2p=1.04\mu_B$. The effective bosonic model, which allows to describe magnetic properties of iron near the magnetic phase transition, is proposed.

DOI: 10.1103/PhysRevB.81.045117 PACS number(s): 75.10.Lp, 75.50.Bb, 75.30.Cr, 71.20.Be

I. INTRODUCTION

The magnetism and its influence to properties of materials attracts a lot of interest since ancient ages, first records can be traced back to Greek philosopher Thales of Miletus and Indian surgeon Sushruta about 600 BC. In particular, the problem of origin of ferromagnetism of iron attracts a lot of attention, despite long time of its investigations.

The d electrons in iron (as well as in many other transition metals) show both, localized and itinerant behavior. According to the Rhodes and Wolfarth criterion, iron is classified as a local-moment system since the ratio of the magnetic moment $2p_{\mathrm{CW}}\mu_B$ corresponding to the effective spin p_{CW} extracted from Curie-Weiss law for susceptibility $\chi=g^2\mu_B^2 p_{\mathrm{CW}}(p_{\mathrm{CW}}+1)/[3(T-T_C)]$ ($g\approx 2$ is the g factor, μ_B is the Bohr magneton, and T_C being the Curie temperature) to the magnetic moment per atom in the ferromagnetic phase, $2p_{\mathrm{CW}}\mu_B/\mu_{\mathrm{exp}}=1.05$ is close to unity (see, e.g., Ref. 1). At the same time, the experimental magnetic moment of iron $\mu_{\mathrm{exp}}=2.2\mu_B$ is not an integer number, which indicates presence of some fraction of itinerant electrons.

Itinerant theory of magnetism of transition metals was pioneered by Stoner, and then became a basis of spin-fluctuation theory by Moriya[1] which was successful to describe weak and nearly ferromagnetic and antiferromagnetic materials. By considering fluctuation corrections to mean field, Moriya theory was able to reproduce nearly Curie-Weiss behavior of magnetic susceptibility and to obtain correct values of transition temperatures of weak or nearly magnetic systems. At the same time, this theory meets serious difficulties when applied to materials with large magnetic moment, such as some transition metals. These materials are expected to be better described in terms of the local-moment picture. In practice, to describe d electrons in transition metals in the semiphenomenological way, the localized-moment (Heisenberg) model is often used. Band-structure calculations of magnetic exchange interaction in iron and nickel show however its non-Heisenberg character at intermediate and large momenta.[2] Using microscopic consideration Mott[3] proposed a two-band model for transition metals with narrow band of d electrons and wide band of s electrons. The polar s-d model, which treats d electrons as localized and s electrons as itinerant was proposed by Shubin and Vonsovski.[4]

First attempts to unify the localized and itinerant pictures of magnetism were performed in Refs. 1 and 5 for the single and degenerate band models, respectively. To unify localized and itinerant approaches to magnetism and find an origin of the formation of local moments, it seems however important to consider the orbital-resolved contributions to one- and two-particle properties. In particular, it was suggested by Goodenough[6] that the electrons with e_g and t_{2g} symmetries may behave very differently in iron: while the former show localized, the latter may show itinerant behavior. The "95% localized model" of iron was proposed by Stearns[7] according to which 95% of d electrons are localized while 5% are itinerant. This idea found its implementation in the "two-band model,"[8] which was considered within the mean-field approach. Later on it was suggested[9,10] that the states at the Van Hove singularities may induce localization of some d-electron states. However, no microscopic evidences for such localization were obtained so far.

The important source of the local-moment formation is strong electronic correlations. In particular, the ferromagnetic state of the one-band strongly correlated Hubbard model, which was shown to be stable for sufficiently large on-site Coulomb repulsion,[11,12] has linear dependence of the inverse susceptibility above transition temperature within the dynamical mean-field theory (DMFT).[12] The role of interband Coulomb interaction and Hund exchange in nondegenerate Hubbard model to reduce the critical intraband Coulomb interaction strength was emphasized in Refs. 13 and 14.

To get insight in the applicability of the above-mentioned proposals to mechanism of local-moment formation in iron, the combination of first-principles[15–17] and model calculations seems necessary. The recently performed combination of local-density approximation (LDA) and DMFT calculations[18] allowed to describe quantitatively correct the magnetization and susceptibility of iron as a function of the reduced temperature T/T_C; in particular, they led to almost linear temperature dependence of the inverse static spin susceptibility above the magnetic transition temperature, which

is similar to the results of model calculations and can be considered as possible evidence for existence of local moments. The estimated magnetic transition temperature appears however twice large than the experimental value $T_C = 1043$ K. The one-particle properties below the transition temperature were addressed in Refs. 19 and 20. To get insight into the mechanism of the formation of local moments and linear dependence of susceptibilities above the Curie temperature it seems however important to study one- and two-particle properties in the *paramagnetic* phase.

To this end we reconsider in the present paper *ab initio* LDA+DMFT calculations, paying special attention to orbital-resolved contributions to one- and two-particle properties. Contrary to previously accepted view that Hund exchange only helps to form ferromagnetic state, we argue that in fact it serves as a main source of formation of local moments in iron, together with the almost absent hybridization between t_{2g} and e_g bands. These two factors yield formation of local moments for the e_g states while t_{2g} states remain more itinerant.

II. *d*-ELECTRON MODEL AND ORBITAL-SELECTIVE MAGNETIC MOMENTS

To discuss the behavior of d electrons in iron let us start from standard multiband Hubbard Hamiltonian,

$$\hat{H}^d = \hat{H}_{\rm kin} + \hat{H}^d_{\rm int} + \sum_{\mathbf{k}} \sum_{mm'\sigma} t_{mm'}(\mathbf{k}) \hat{c}^\dagger_{\mathbf{k}m\sigma} \hat{c}_{\mathbf{k}m'\sigma} + \frac{1}{2} \sum_i \sum_{\{m\}\sigma\sigma'} \langle m,m'|V_{ee}|m'',m'''\rangle \hat{c}^\dagger_{im\sigma} \hat{c}^\dagger_{im'\sigma'} \hat{c}_{im''\sigma} \hat{c}_{im'''\sigma'}, \tag{1}$$

where the first term represents a kinetic contribution to Hamiltonian and the second one is an interaction part. $c^\dagger_{\mathbf{k}m\sigma}(c_{\mathbf{k}m\sigma})$ are creation (annihilation) operators for electron with respective quantum indices $|\mathbf{k}m\sigma\rangle$ and $c^\dagger_{im\sigma}$ is a Fourier image in real space, $t_{mm'}(\mathbf{k})$ is a dispersion, and $\langle m,m'|V_{ee}|m'',m'''\rangle$ is a Coulomb interaction matrix. For the sake of simplicity we assume that orbital index m runs over the correlated d orbitals only.

Keeping a density-density and spin-flip terms in the interacting part of above Hamiltonian [Eq. (1)] and assuming a simple parameterization of the interaction matrix with the intraorbital Coulomb interaction, $U=\langle m,m|V_{ee}|m,m\rangle$, the interorbital Coulomb interaction, $U'=\langle m,m'|V_{ee}|m,m'\rangle$, and Hund's exchange, $I=\langle m,m'|V_{ee}|m',m\rangle$ one can rewrite the interaction as

$$H^d_{\rm int} = U \sum_{im} \hat{n}_{im\uparrow}\hat{n}_{im\downarrow} + \left(U' - \frac{I}{2}\right) \sum_{i,m<m',\sigma\sigma'} \hat{n}_{im\sigma}\hat{n}_{im'\sigma'} - 2I \sum_{i,m<m'} \hat{\mathbf{s}}_{im}\hat{\mathbf{s}}_{im'}, \tag{2}$$

where m,m runs over all d-orbital indices and

$$\hat{n}_{im\sigma} = \hat{c}^\dagger_{im\sigma}\hat{c}_{im\sigma},$$

$$\hat{\mathbf{s}}_{im} = \frac{1}{2}\sum_{\sigma\sigma'} \hat{c}^\dagger_{im\sigma}\boldsymbol{\sigma}_{\sigma\sigma'}\hat{c}_{im\sigma'},$$

$\boldsymbol{\sigma}$ are the Pauli matrices.

Generically, the Coulomb interaction yields loss of coherence of corresponding electronic states. It will be shown in Sec. III, that electrons in weakly hybridized t_{2g} and e_g orbitals behave very differently with respect to the Coulomb interaction. While the behavior of t_{2g} electrons remains Fermi liquidlike, e_g electrons form a non-Fermi-liquid states that implies formation of local moments. Magnetic properties of the resulting system can be then understood in terms of an effective model, containing spins of local and itinerant electron subshells.

Splitting in Eq. (2) contributions of e_g and t_{2g} electrons and neglecting hybridization between them (which will be shown to be small in Sec. III A), we can rewrite the Hamiltonian (1) as

$$\hat{H}^d = \hat{H}^{t_{2g}} + \hat{H}^{e_g} - 2I \sum_{i,m\in t_{2g}} \hat{\mathbf{S}}_i\hat{\mathbf{s}}_{im} + \left(U' - \frac{I}{2}\right) \sum_{i,\sigma,m\in t_{2g}} \hat{N}_i\hat{n}_{im\sigma}, \tag{3}$$

where $\hat{H}^{t_{2g}}$ and $\hat{H}^{e_g}$ are the parts of Hamiltonian (1) acting on the t_{2g} and e_g orbitals, respectively, $\hat{\mathbf{S}}_i = \Sigma_{m\in e_g}\hat{\mathbf{s}}_{im}$ and $\hat{N}_i = \Sigma_{m\in e_g}\hat{n}_{im}$. Note that operators $\hat{\mathbf{S}}_i$ do not generically describe fully local moments but will be shown to have properties close to those of local moments due to Hund exchange interaction. Below after considering the results of band-structure calculations, we discuss the effect of interaction in Eq. (3) within DMFT and its implications for the effective model.

III. FIRST-PRINCIPLES CALCULATIONS FOR IRON

A. Band-structure results

Iron crystallizes in body-centered-cubic structure below 1183 K and has the lattice parameter $a=2.8664$ Å at room temperature.[21] Band-structure calculations have been carried out in LDA approximation[22] within tight-binding-linear muffin-tin orbital-atomic spheres approximation framework.[23] The von Barth-Hedin local exchange-correlation potential was used.[24] Primitive reciprocal translation vectors were discretized into 12 points along each direction which leads to 72 $\mathbf{k}$ points in irreducible part of the Brillouin zone.

Total and partial densities of states (DOSs) are presented in Fig. 1. The contribution of a wide s band is shown by (red) dots and spreads from −8.5 eV to energies well above the Fermi level (at zero energy); t_{2g} and e_g states [(green) dashed and (blue) dot-dashed] span energy region from −5 to 1 eV approximately. In spite of almost equal bandwidths of t_{2g} and e_g states they are qualitatively different. Former states are distributed more uniformly over the energy range while the later one have a large peak located at the Fermi energy.

The contributions of t_{2g} and e_g orbitals to the band structure of iron are presented in Fig. 2 (left and right panels, respectively). The states contributing to the Van Hove singu-

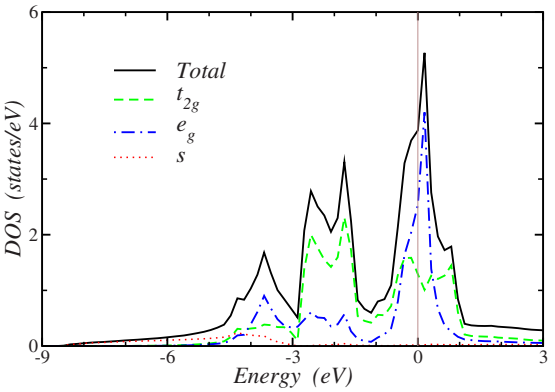

FIG. 1. (Color online) Iron density of states obtained within LDA approximation. Total DOS is shown by solid (black) line. Partial t_{2g}, e_g, and s DOSs are shown by (green) dashed, (blue) dot-dashed, and (red) dot lines, respectively.

larity near the Fermi energy are of mostly e_g symmetry. As it was argued in Refs. 10 and 25, despite the three-dimensional character of the band structure, the lines of Van Hove singularities, which due to symmetry reasons can easily occur along the Γ-N direction, produce a peak in the density of states. In fact, this singularity is actually a part of the flat band going along Γ-N-P-Γ directions. On the other hand, t_{2g} bands do not have a flatness close to the Fermi level. These peculiarities of the band structure and absence of direct hybridization between t_{2g} and e_g states suggest that the t_{2g} and e_g electrons may behave very differently when turning on on-site Coulomb interaction.

B. DMFT calculations

In order to take into account correlation effects in $3d$ shell of α-iron the LDA+DMFT method was applied (for detailed description of the computation scheme see Ref. 26). We use the Hamiltonian of Hubbard type as in Eq. (1) with the kinetic term containing all s-p-d states and the interaction part with density-density contributions for d electrons only,

$$\hat{H}_{\text{int}} = \frac{1}{2}\sum_{imm'\sigma}\{U_{mm'}\hat{n}_{im\sigma}\hat{n}_{im'\bar{\sigma}} + (U_{mm'} - I_{mm'})\hat{n}_{im\sigma}\hat{n}_{im'\sigma}\}, \tag{4}$$

where $U_{mm'} \equiv \langle m,m'|V_{ee}|m,m'\rangle$ and $I_{mm'} \equiv \langle m,m'|V_{ee}|m',m\rangle$. Regarding interaction between d electrons, the model

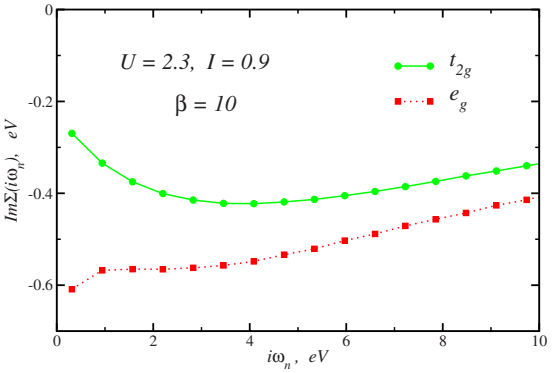

FIG. 3. (Color online) The imaginary part of self-energy for t_{2g} (green solid line) and e_g states (red dotted line) plotted on the Matsubara (imaginary) energy grid.

(B) serves as a simplified version of the model (1) since it does not contain transverse components of the Hund exchange and pair-hopping term.

The Coulomb interaction parameter value $U=2.3$ eV and the Hund's parameter $I=0.9$ eV used in our work are the same as in earlier LDA+DMFT calculations by Lichtenstein *et al.*[18] To treat a problem of formation of local moments we consider paramagnetic phase. The effective impurity model for DMFT was solved by quantum-Monte-Carlo (QMC) method with the Hirsch-Fye algorithm.[27] Calculations were performed for the value of inverse temperature $\beta=10$ eV^{-1} which is close to the $\alpha \rightarrow \gamma$ transition temperature. Inverse temperature interval $0<\tau<\beta$ was divided in 100 slices. 4 million QMC sweeps were used in self-consistency loop within LDA+DMFT scheme and up to 12 million of QMC sweeps were used to calculate spectral functions.

In Fig. 3 the imaginary parts of self-energy of t_{2g} and e_g electrons are shown on the imaginary frequency axis. One can clearly see that the behavior of $\Im\Sigma(i\omega_n)$ at low energies is qualitatively different for different orbitals. While $\Im\Sigma(i\omega_n)$ for t_{2g} states has a Fermi-liquidlike behavior with the quasiparticle weight $Z=0.86$, zero energy outset $\Re\Sigma(0) \simeq 1.1$ eV, and damping $\Im\Sigma(0)=-0.22$ eV, the $\Im\Sigma(i\omega_n)$ for e_g orbitals has a divergentlike shape indicating a loss of coherence regime. As it will be shown in the Sec. III C, the latter states form local magnetic moments. This fact affords a ground for separation of the iron d states onto two subsystems; more localized e_g states and itinerant t_{2g} states. Contrary to the picture proposed in Ref. 9, we find not only localization of

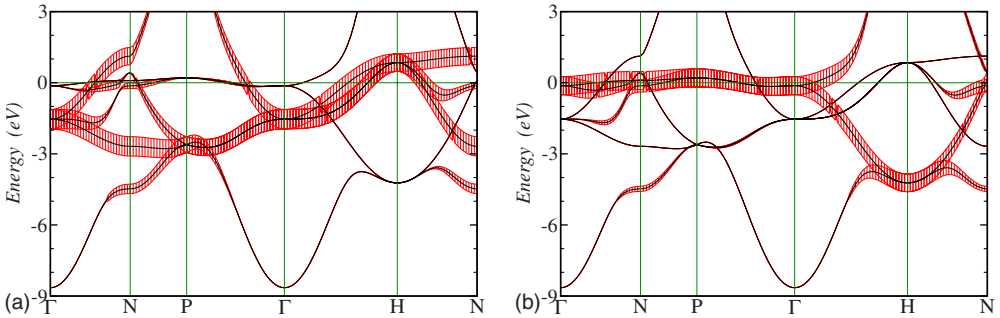

FIG. 2. (Color online) The band structure of Fe along high-symmetry lines in the Brillouin zone obtained within LDA approximation. The contribution of t_{2g} (left panel) and e_g (right panel) states is shown with fat (red) lines.

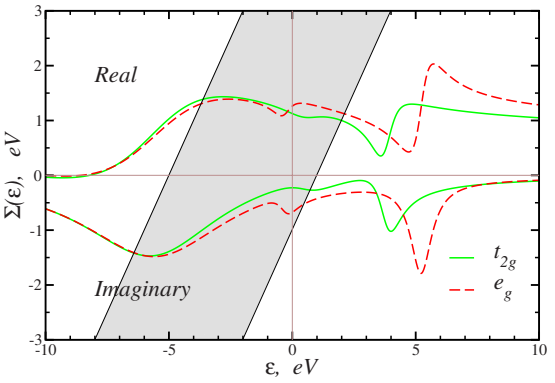

FIG. 4. (Color online) The self-energy for t_{2g} (green solid line) and e_g states (red dashed line) plotted on the real energy axis. Straight lines $\Sigma=\omega+E_{\min,\max}$, which bound shaded area, correspond to the bottom ($E_{\min}$) and top ($E_{\max}$) of the band.

electrons, contributing to the Van Hove singularity states but also most part of e_g electrons is expected to form local moments. The features observed for e_g states are similar to those observed near Mott metal-insulator transition[28] (see also the results on the real axis below in Fig. 4), although in our case non-Fermi-liquid behavior touches only part of the states and the metal-insulator transition does not happen. We have verified that the obtained results depend very weakly on U in the range from 2 to 6 eV while switching off (or reducing) I immediately suppresses non-Fermi-liquid contributions. Therefore, Hund exchange serves as a major source of local-moment formation of e_g states.

Figure 4 shows the resulting behavior of real and imaginary parts of the self-energy of different orbitals on the real axis. To make an analytic continuation of the complex function we used Pade approximation method[29] with energy mesh containing both, low- and high-energy frequencies. To satisfy high-frequency behavior the equality of the first three moments of function calculated on the real and imaginary axes was fulfilled. Altogether this procedure guarantees an accurate description of the function close to Fermi level and at high energy. In compliance with the observations from imaginary axis, $\Re\Sigma(\omega)$ has slightly negative slope for t_{2g} states, accompanied by the maximum of $\Im\Sigma(\omega)$ at the Fermi level while for e_g states $\Re\Sigma(\omega)$ has positive slope and $\Im\Sigma(\omega)$ is minimal at the Fermi level. The characteristic energy scale for the observed non-Fermi-liquid behavior is on the order of 1 eV, i.e., the Hund exchange parameter, which is too small to produce Hubbard subbands, see straight lines in Fig. 4. Seemingly, the observed features represent stronger breakdown of the Fermi-liquid behavior than $\Im\Sigma\propto T^{1+\alpha}$ obtained earlier in the three-band Hubbard model.[30]

Partial densities of states obtained in paramagnetic LDA+DMFT calculation for t_{2g} and e_g electrons are presented in Fig. 5. The LDA+DMFT densities of states are slightly narrower than the LDA counterparts implying weak correlation effects. One can observe that peak of e_g density of states observed in LDA approach is suppressed in LDA+DMFT calculation and split into two peaks at −0.3 and 0.5 eV due to non-Fermi-liquid behavior of these states. As discussed above, this splitting should be distinguished from the Hubbard subbands formation near Mott metal-insulator transition, e.g., due to much smaller energy scale, which is of the order of Hund exchange interaction. The shape of t_{2g} density of states in LDA+DMFT approach resembles the LDA result with smearing of the peaky structures of density of states by correlations.

C. DMFT spin susceptibility

To discuss the effect of the nonquasiparticle states of e_g electrons on magnetic properties we consider imaginary-time dependence of the impurity spin susceptibilities,

$$\chi_{e_g}(\tau)=\sum_{mm'\in e_g}\langle T[\hat{s}^z_{im}(\tau)\hat{s}^z_{im'}(0)]\rangle=\langle T[\hat{S}^z_i(\tau)\hat{S}^z_i(0)]\rangle,$$

$$\chi_{t_{2g}}(\tau)=\sum_{mm'\in t_{2g}}\langle T[\hat{s}^z_{im}(\tau)\hat{s}^z_{im'}(0)]\rangle$$

obtained within DMFT. The results for the time dependence of $\chi_{e_g}(\tau)$, $\chi_{t_{2g}}(\tau)$, and total impurity susceptibility $\chi(\tau)$ for $U=2.3$ eV and $I=0.9$ eV are shown on the insets of Fig. 6. One can see that the dependence $\chi_{e_g}(\tau)$ on imaginary time is more flat than $\chi_{t_{2g}}(\tau)$. This fact reflects the formation of local moments for e_g electrons, which would correspond to fully time-independent $\chi_{e_g}(\tau)$. Switching off I suppresses susceptibility at the flat parts, destroying therefore local moments.

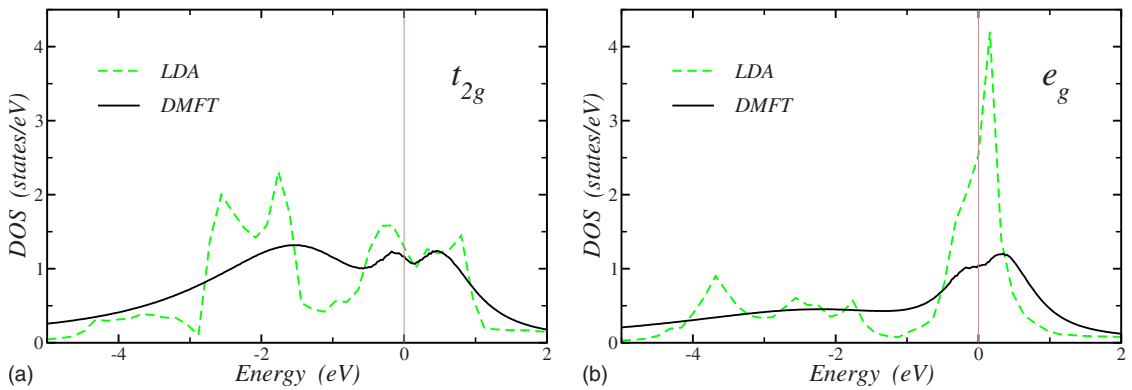

FIG. 5. (Color online) The iron t_{2g} (left panel) and e_g (right panel) partial density of states obtained within LDA+DMFT method (black solid lines) compared with LDA DOS (green dashed lines).

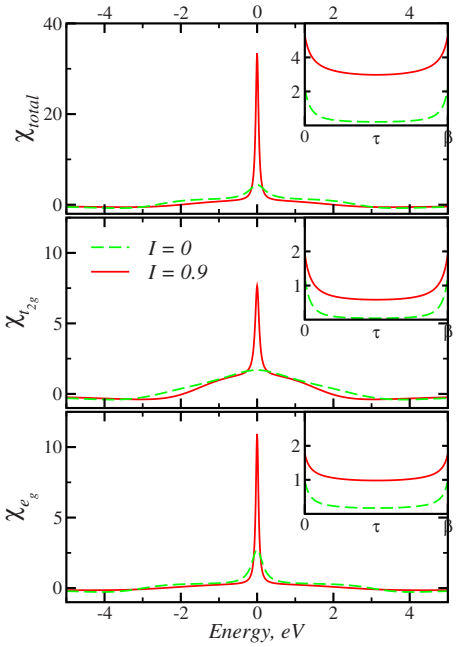

FIG. 6. (Color online) Impurity spin susceptibility for the value of Coulomb interaction, $U=2.3$ eV, inverse temperature, $\beta=10$ eV^{-1} and Hund coupling, $I=0$ (green dashed) and 0.9 eV (red solid) plotted on the real axis. Total impurity spin susceptibility and t_{2g} and e_g contributions are shown from top to bottom. The insets show the corresponding imaginary-time data.

The observed behavior as a function of imaginary time is also reflected as a function of real frequency (Fig. 6). One can see that flat part of the imaginary-time dependence of the susceptibilities yields peak in the real frequency dependence, which is mostly pronounced for e_g states. The peak contributions are similar to the frequency dependence of susceptibility of an isolated spin p (note neglecting spatial correlations in DMFT), $\chi(i\omega_n)=g^2\mu_B^2 p(p+1)/(3T)\delta_{n,0}$ and show presence of local moment for e_g states. For t_{2g} states we observe mixed behavior with peak contribution transferred from e_g states via Hund exchange (see Sec. IV) and incoherent background, originating from t_{2g} itinerant states. These peaky contributions to susceptibilities disappear with switching off I, which shows once more that Hund exchange is the major source of the local-moment formation.

One of the most transparent characteristic features of the local-moment formation is the fulfillment of the Curie-Weiss law for the temperature dependence of the susceptibility. In particular, in the limit of local moments the magnetic moment μ_{CW} extracted from Curie-Weiss law is expected to be approximately equal to the magnetic moment in the symmetry-broken phase. The obtained temperature dependence of the local (impurity) susceptibilities is shown in Fig. 7 (the temperature dependence of lattice susceptibilities will be presented elsewhere). One can see that the inverse susceptibility of e_g states obeys Curie law with $p_{\mathrm{CW}}(e_g)=0.52$. The inverse susceptibility of t_{2g} states also shows approximately linear temperature dependence with $p_{\mathrm{CW}}(t_{2g})\simeq 0.7$. The Curie law for the total susceptibility yields $p_{\mathrm{CW}}=1.16$, the corresponding Curie constant $\mu_{eff}^2\equiv g^2\mu_B^2 p_{\mathrm{CW}}(p_{\mathrm{CW}}+1)=10\mu_B^2$ is in good agreement with experimental data and earlier calculations of the lattice susceptibility in the paramagnetic phase.[18] Note close proximity of obtained value $p_{\mathrm{CW}}(e_g)$ to 1/2.

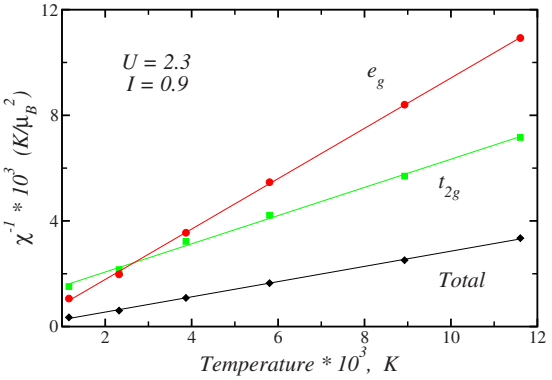

FIG. 7. (Color online) Temperature dependence of inverse of the local spin susceptibility. Total spin susceptibility and orbital-resolved contributions are presented by (black) diamonds, (green) squares (t_{2g}), and (red) circles (e_g), respectively. Lines are least-squares fitting to the original data.

IV. EFFECTIVE MODEL

The formation of local moments by e_g electrons makes the model (3) reminiscent of the multiband generalization of s-d exchange model, supplemented by Coulomb interaction in t_{2g} bands. The s-d model was suggested by Shubin and Vonsovski to describe magnetism of rare-earth elements and some transition-metal compounds.[4] Differently to its original formulation, both itinerant and localized states in the model (3) correspond to d electrons, with the t_{2g}- and e_g-orbital symmetry, respectively, and Coulomb interaction in t_{2g} band is present.

Similarly to the diagram technique for the s-d model,[31] the contribution of the "wideband" t_{2g} electrons can be treated perturbatively. Moreover, we can integrate out electronic degrees of freedom for t_{2g} band and pass to purely bosonic model in a spirit of Moriya theory. Specifically, we introduce new variables $\mathbf{t}_q^m$ for spins of t_{2g} electrons by decoupling interaction terms in $H_{t_{2g}}$ via Hubbard-Stratonovich transformation and summing contributions from different spin directions (the double counted terms are supposed to be substracted). We treat only magnetic terms of the interaction since we are interested in magnetic properties. The Lagrangian, which is obtained by Hubbard-Stratonovich transformation after expansion in the Coulomb interaction between t_{2g} states and Hund exchange can be represented in the form

$$L = L_{e_g} + \sum_{q,mm'} [R^{-1}_{mm'}\mathbf{t}_q^m\mathbf{t}_{-q}^{m'} - \Pi_q^{mm'}(\mathbf{t}_q^m + 2I\mathbf{S}_q)(t_{-q}^{m'} + 2I\mathbf{S}_{-q})]$$
$$+ \sum_{q_i,m_i} \Lambda^{mm'm''m'''}_{q_1q_2q_3,abcd}(\mathbf{t}_{q_1}^m + 2I\mathbf{S}_{q_1})_a(\mathbf{t}_{q_2}^{m'} + 2I\mathbf{S}_{q_2})_b(\mathbf{t}_{q_3}^{m''} + 2I\mathbf{S}_{q_3})_c$$
$$\times (\mathbf{t}^{m'''}_{-q_1-q_2-q_3} + 2I\mathbf{S}_{-q_1-q_2-q_3})_d, \quad (5)$$

where $R_{mm'}=U\delta_{mm'}+J(1-\delta_{mm'})$, the sums over band indices are taken over t_{2g} states only, $a,b,c,d=x,y$, or z,

$$\Pi_q^{mm'} = -\sum_k G_k^{mm'} G_{k+q}^{m'm},$$

$$\Lambda_{q_1q_2q_3,abcd}^{mm'm''m'''} = \frac{1}{16}\mathrm{Tr}(\sigma^a\sigma^b\sigma^c\sigma^d) \times \sum_k G_k^{mm'} G_{k+q_1}^{m'm''} G_{k+q_1+q_2}^{m''m'''} G_{k+q_1+q_2+q_3}^{m'''m}. \quad (6)$$

$G_k^{mm'}$ is the matrix of the (interacting) t_{2g}-electron Green's functions, and we use the four-vector notations $q=(i\omega,\mathbf{q})$, etc. Due to nonquasiparticle nature of e_g electrons, the interaction acting on e_g electrons and mixed e_g-t_{2g} terms in the interaction need not be decoupled; the former is supposed to be accounted within a nonperturbative approach, e.g., DMFT while the latter are treated perturbatively. In dynamical mean-field theory quantities $\Pi_q^{mm'}$ and $\Lambda_{q_1q_2q_3,abcd}^{mm'm''m'''}$ for generic momenta are the functions of frequencies only.

The Lagrangian (4) can be viewed as the generalization of the standard ϕ^4 model of the magnetic transition of itinerant electrons[1,32] to the case of presence of nearly local moments. For the susceptibilities of t_{2g} and e_g electrons, and mixed t_{2g}-e_g susceptibility υ_q we obtain up to second order in I,

$$\begin{pmatrix} (R\chi_{q,t_{2g}}+I)R & \upsilon_q R \\ \upsilon_q R & \chi_{q,e_g} \end{pmatrix} = \begin{pmatrix} (\chi^0_{q,t_{2g}})^{-1}+\Lambda*\chi^0_{t_{2g}}+4I^2\Lambda*\chi^0_{e_g} & -2I\Pi_q \\ -2I\Pi_q & (\chi^0_{q,e_g})^{-1}-4I^2\Pi_q+4I^2\Gamma^{(4)}*\chi^0_{t_{2g}} \end{pmatrix}^{-1}, \quad (7)$$

where $\chi^0_{q,t_{2g}}=(R^{-1}_{mm'}-\Pi_q^{mm'})^{-1}$ is the random-phase approximation spin susceptibility of t_{2g} band, $\chi^0_{q,e_g}=\langle \mathbf{S}_q\mathbf{S}_{-q}\rangle_{e_g}/3$ is the bare susceptibility of e_g band, evaluated with L_{e_g},

$$\Gamma^{(4),abcd}_{q_1q_2q_3} = \langle S^a_{q_1}S^b_{q_2}S^c_{q_3}S^d_{-q_1-q_2-q_3}\rangle_{e_g} - \chi^0_{q_1,e_g}\chi^0_{q_3,e_g}\delta_{q_1,-q_2}\delta_{a,b}\delta_{c,d} - \chi^0_{q_1,e_g}\chi^0_{q_2,e_g}(\delta_{q_2,-q_3}\delta_{b,c}\delta_{a,d}+\delta_{q_1,-q_3}\delta_{a,c}\delta_{b,d}) \quad (8)$$

is the four-spin Green's function, and $*$ denote the convolution of momenta, frequency, and band indices. Again, within DMFT the quantities $\chi^0_{e_g,q}$ and $\Gamma^{(4),abcd}_{q_1q_2q_3}$ are only frequency dependent.

The form of the susceptibilities [Eq. (7)] allows, in particular, to understand the mechanism of fulfillment the Curie law for local susceptibilities of both, t_{2g} and e_g electrons and their frequency dependence. While e_g electrons form local moments, $\chi^0_{e_g}$ becomes almost static and shows inverse linear temperature dependence, similar to that obtained in the Heisenberg model. The contribution $4I^2\Pi_q$ corresponds to Ruderman-Kittel-Kasuya-Yoshida interaction and expected to be weakly temperature dependent. Presumably small contribution $4I^2\Gamma^{(4)}*\chi^0_{t_{2g}}$ can also add some linear in temperature dynamic contribution to the inverse susceptibility of e_g electrons. Note that within DMFT this contribution is accounted only in average with respect to momenta, and does not allow to resolve peculiar physics, which arises due to contribution of small momenta (forward scattering). The convolutions $\Lambda*\chi_{t_{2g}}$ and $4I^2\Lambda*\chi_{e_g}$ determine the contributions to the susceptibility of t_{2g} electrons from interaction within t_{2g} band and between t_{2g} and e_g bands, respectively, and become also linear functions of temperature similarly to the Moriya theory (where they correspond to the so-called λ correction). These contributions are however incoherent due to complicated frequency dependence of Λ. Finally, the terms $I\Pi_q$ mix these two (coherent and incoherent) contributions to the susceptibilities due to interorbital Hund exchange and Coulomb interaction in t_{2g} band.

Therefore, the model (5) allows to understand main features of frequency and temperature dependences of susceptibilities, observed in the DMFT solution. The derivation of the bosonic model and susceptibilities [Eq. (7)] can further serve as a basis for obtaining nonlocal corrections to the results of dynamic mean-field theory, e.g., in a spirit of dynamic vertex approximation.[37,38]

V. CONCLUSION

We have discussed the origin of the formation of local moments in iron, which is due to the localization of e_g electrons. In particular, we observe non-Fermi-liquid behavior in e_g but not t_{2g} band. This mechanism is very similar to the concept of orbital-selective Mott transition, which was earlier introduced in Ref. 33 for $Ca_{2-x}Sr_xRuO_4$. Although a possibility of a separate Mott transition in narrow bands (in the presence of hybridization with a wideband) was questioned by Liebsch,[34] the recent high-precision QMC studies of the two-band model have confirmed this possibility.[35] The features of the self-energy at the imaginary frequency axis, obtained in present study, are also similar to those discussed in the context of orbital-selective Mott transition,[36] where the enhanced damping of itinerant electrons, as well as crucial role of Hund exchange was observed. In our case, obtained non-Fermi-liquid behavior of e_g electrons yields peak in the frequency dependence of spin-spin correlation function and linear temperature dependence of the magnetic susceptibility of e_g electrons with $p_{\mathrm{CW}}=0.52$, both being characteristic features of local moments, formed in e_g band.

The formulated spin-fluctuation approach allows to describe thermodynamic properties in the spin-symmetric phase. To describe symmetry-broken phase, as well as prox-

imity to the magnetic transition temperature, nonlocal (in particular, long-range) correlations beyond DMFT are expected to become important. These correlations are also likely to reduce the DMFT transition temperature closer to its experimental value. Although the systematic treatment of the nonlocal long-range correlations in the strongly correlated systems is applied currently mainly to the one-band model,[37–40] it was shown recently that nonlocal corrections substantially reduce the magnetic transition temperature from its DMFT value.[38] Future investigations of nonlocal corrections in multiband models, together with evaluation of thermodynamic properties, have to be performed.

The presented approach can be also helpful to analyze the electron structure of γ-iron and mechanism of the structural α-γ transformation of iron.[41] Existing approaches to this problem often start from the Heisenberg model, where the short-range magnetic order in γ phase was suggested as the origin of the α-γ transformation.[42] This picture may need reinvestigation from the itinerant point of view. The presented approach can be useful also for other substances, containing both, local moments and itinerant electrons.

ACKNOWLEDGMENTS

The authors thank Jan Kuneš for providing his DMFT (QMC) computer code used in our calculations. Support by the Russian Foundation for Basic Research under Grants No. RFFI-07-02-00041, No. RFFI-07-02-01264-a, and No. RFFI-08-02-91953-NNIO-a, Civil Research and Development Foundation together with the Russian Ministry of Science and Education through program Y4-P-05-15, Federal Agency for Science and Innovations under Grant No. 02.740.11.0217, Dynasty Foundation, the fund of the President of the Russian Federation for the support for scientific schools under Grant No. NSH 1941.2008.2, the Programs of Presidium of Russian Academy of Science "Quantum microphysics of condensed matter" (No. 7) and "Physics of strongly compressed matter," and Grant No. 62-08-01 (by "MMK," "Ausferr," and "Intels") is gratefully acknowledged.

[1] T. Moriya, *Spin Fluctuations in Itinerant Electron Magnetism* (Springer-Verlag, Berlin, 1985).
[2] V. A. Gubanov, A. I. Lichtenstein, and A. V. Postnikov, *Magnetism and Electronic Structure of Crystals* (Springer-Verlag, Berlin, 1992).
[3] N. F. Mott, Proc. Phys. Soc. **47**, 571 (1935).
[4] S. P. Shubin and S. V. Vonsovski, Proc. R. Soc. London **A145**, 159 (1934); S. V. Vonsovski, *Magnetism* (Wiley, New York, 1974).
[5] J. Hubbard, Phys. Rev. B **19**, 2626 (1979); **20**, 4584 (1979).
[6] J. B. Goodenough, Phys. Rev. **120**, 67 (1960).
[7] M. B. Stearns, Phys. Rev. B **8**, 4383 (1973).
[8] R. Mota and M. D. Coutinho-Filho, Phys. Rev. B **33**, 7724 (1986).
[9] V. Yu. Irkhin, M. I. Katsnelson, and A. V. Trefilov, J. Phys.: Condens. Matter **5**, 8763 (1993).
[10] S. V. Vonsovskii, M. I. Katsnelson, and A. V. Trefilov, Fiz. Met. Metalloved. **76** (3), 3 (1993); **76** (4), 3 (1993).
[11] T. Hanisch, Götz S. Uhrig, and E. Müller-Hartmann, Phys. Rev. B **56**, 13960 (1997).
[12] M. Ulmke, Eur. Phys. J. B **1**, 301 (1998); T. Obermeier, T. Pruschke, and J. Keller, Phys. Rev. B **56**, R8479 (1997); J. Wahle, N. Blümer, J. Schlipf, K. Held, and D. Vollhardt, *ibid.* **58**, 12749 (1998).
[13] K. Held and D. Vollhardt, Eur. Phys. J. B **5**, 473 (1998); D. Vollhardt, N. Blümer, K. Held, M. Kollar, J. Schlipf, M. Ulmke, J. Wahle, *Advances in Solid State Physics* (Vieweg, Wiesbaden, 1999), Vol. 38, p. 383; D. Vollhardt, N. Blümer, K. Held, and M. Kollar, *Lecture Notes in Physics* (Springer, New York, 2001), Vol. 580, p. 191.
[14] S. Sakai, R. Arita, and H. Aoki, Phys. Rev. Lett. **99**, 216402 (2007).
[15] M. F. Manning, Phys. Rev. **63**, 190 (1943).
[16] J. Callaway, Phys. Rev. **99**, 500 (1955).
[17] E. Abate and M. Asdente, Phys. Rev. **140**, A1303 (1965).
[18] A. I. Lichtenstein, M. I. Katsnelson, and G. Kotliar, Phys. Rev. Lett. **87**, 067205 (2001).
[19] M. I. Katsnelson and A. I. Lichtenstein, J. Phys.: Condens. Matter **11**, 1037 (1999); A. Grechnev, I. Di Marco, M. I. Katsnelson, A. I. Lichtenstein, J. Wills, and O. Eriksson, Phys. Rev. B **76**, 035107 (2007).
[20] M. I. Katsnelson and A. I. Lichtenstein, Phys. Rev. B **61**, 8906 (2000); J. Phys.: Condens. Matter **16**, 7439 (2004).
[21] *Constitution of Binary Alloys*, edited by M. Hansen (McGraw-Hill, New York 1958).
[22] R. O. Jones and O. Gunnarsson, Rev. Mod. Phys. **61**, 689 (1989).
[23] O. K. Andersen and O. Jepsen, Phys. Rev. Lett. **53**, 2571 (1984).
[24] U. von Barth and L. Hedin, J. Phys. C **5**, 1629 (1972).
[25] R. Maglic, Phys. Rev. Lett. **31**, 546 (1973).
[26] V. I. Anisimov, D. E. Kondakov, A. V. Kozhevnikov, I. A. Nekrasov, Z. V. Pchelkina, J. W. Allen, S.-K. Mo, H.-D. Kim, P. Metcalf, S. Suga, A. Sekiyama, G. Keller, I. Leonov, X. Ren, and D. Vollhardt, Phys. Rev. B **71**, 125119 (2005).
[27] J. E. Hirsch and R. M. Fye, Phys. Rev. Lett. **56**, 2521 (1986).
[28] R. Bulla, T. A. Costi, and D. Vollhardt, Phys. Rev. B **64**, 045103 (2001).
[29] H. J. Vidberg and J. W. Serene, J. Low Temp. Phys. **29**, 179 (1977).
[30] P. Werner, E. Gull, M. Troyer, and A. J. Millis, Phys. Rev. Lett. **101**, 166405 (2008).
[31] Yu. A. Izyumov, F. A. Kassan-Ogly, and Yu. N. Skryabin, *Field Methods in the Theory of Ferromagnetism* (Nauka, Moscow, 1974); Yu. A. Izyumov and Yu. N. Skryabin, *Statistical Mechanics of Magnetically Ordered Substances* (Consultants Bureau, New York, 1988).
[32] J. A. Hertz, Phys. Rev. B **14**, 1165 (1976).
[33] V. I. Anisimov, I. A. Nekrasov, D. E. Kondakov, T. M. Rice, and M. Sigrist, Eur.Phys. J. B **25**, 191 (2002).
[34] A. Liebsch, Europhys. Lett. **63**, 97 (2003); Phys. Rev. Lett. **91**,

226401 (2003); Phys. Rev. B **70**, 165103 (2004).
[35] C. Knecht, N. Blümer, and P.G.J. van Dongen, Phys. Rev. B **72**, 081103(R) (2005).
[36] S. Biermann, L. de Medici, and A. Georges, Phys. Rev. Lett. **95**, 206401 (2005); L. de' Medici, S. R. Hassan, M. Capone, and X. Dai, *ibid.* **102**, 126401 (2009).
[37] A. Toschi, A. A. Katanin, and K. Held, Phys. Rev. B **75**, 045118 (2007); K. Held, A. A. Katanin, and A. Toschi, Prog. Theor. Phys. **176**, 117 (2008).
[38] A. A. Katanin, A. Toschi, and K. Held, Phys. Rev. B **80**, 075104 (2009).
[39] A. N. Rubtsov, M. I. Katsnelson, and A. I. Lichtenstein, Phys. Rev. B **77**, 033101 (2008); S. Brener, H. Hafermann, A. N. Rubtsov, M. I. Katsnelson, and A. I. Lichtenstein, *ibid.* **77**, 195105 (2008); A. N. Rubtsov, M. I. Katsnelson, A. I. Lichtenstein, and A. Georges, *ibid.* **79**, 045133 (2009).
[40] C. Slezak, M. Jarrell, Th. Maier, and J. Deisz, J. Phys.: Condens. Matter **21**, 435604 (2009).
[41] See, e.g., O. N. Mryasov, V. A. Gubanov, and A. I. Liechtenstein, Phys. Rev. B **45**, 12330 (1992); H. C. Herper, E. Hoffmann, and P. Entel, *ibid.* **60**, 3839 (1999); S. V. Okatov, A. R. Kuznetsov, Yu. N. Gornostyrev, V. N. Urtsev, and M. I. Katsnelson, *ibid.* **79**, 094111 (2009).
[42] A. N. Ignatenko, A. A. Katanin, and V. Yu. Irkhin, JETP Lett. **87**, 555 (2008).